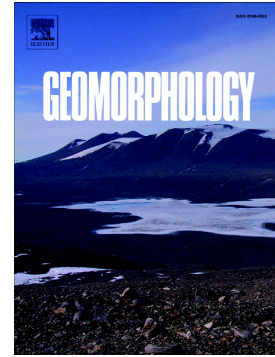


Journal Pre-proof

Earthquake-related speleothem damages: Observations from the 2008 Mw 7.9 Wenchuan, China

Xue-qin Zhao, Fu-dong Wang, Sophie Verheyden, Jing Liu-zeng, Gang Zhang



PII: S0169-555X(20)30102-1

DOI: <https://doi.org/10.1016/j.geomorph.2020.107130>

Reference: GEOMOR 107130

To appear in: *Geomorphology*

Received date: 30 January 2019

Revised date: 26 February 2020

Accepted date: 27 February 2020

Please cite this article as: X.-q. Zhao, F.-d. Wang, S. Verheyden, et al., Earthquake-related speleothem damages: Observations from the 2008 Mw 7.9 Wenchuan, China, *Geomorphology*(2020), <https://doi.org/10.1016/j.geomorph.2020.107130>

This is a PDF file of an article that has undergone enhancements after acceptance, such as the addition of a cover page and metadata, and formatting for readability, but it is not yet the definitive version of record. This version will undergo additional copyediting, typesetting and review before it is published in its final form, but we are providing this version to give early visibility of the article. Please note that, during the production process, errors may be discovered which could affect the content, and all legal disclaimers that apply to the journal pertain.

© 2020 Published by Elsevier.

Earthquake-related speleothem damages: observations from the 2008 Mw 7.9 Wenchuan, China

Xue-qin Zhao^{a,b,c*}, Fu-dong Wang^a, Sophie Verheyden^b, Jing Liu-zeng^c, Gang Zhang^a

a. Institute of Environment and Resources, Southwest University of Science and
Technology, Mianyang, China

b. Analytical, Environmental & Geo-Chemistry, Department of Chemistry, Faculty
of Sciences, Vrije Universiteit Brussels, Brussels, Belgium

c. State Key Laboratory of Earthquake Dynamics, Institute of Geology, China Earth
quake Administration, Beijing, China

Abstract

A speleoseismological study has been conducted at over a dozen cave sites along the Longmen Shan fault zone of the eastern Qinghai-Tibet Plateau. The aim was to assess the damage inflicted on speleothems by the Mw 7.9 Wenchuan earthquake. Results show that the earthquake led to either partial or complete collapse of the caves. 'Soda straws' are shown to be particularly vulnerable to earthquake damage, but statistical analyses indicate that the spindle and slender shapes are also very likely to break. Cave depth is also shown to play an important role in the fracture development during the earthquake. The measured orientations of fallen stalactites are preferentially aligned to the coseismic surface offset peaks and therefore to the direction of earthquake wave propagation. Several such damaged speleothems resulting from sudden co-seismic movements were observed. The direction of ceiling (hanging wall) movement caused by the Wenchuan earthquake is NW-NNW,

* Corresponding author: X-Q Zhao (zxqch@sina.com)

consistent with block motion on the footwall of the Yingxiu-Beichuan fault. We inferred that the faults in the caves were not co-seismic structures of the Wenchuan earthquake; but instead they are likely normal faults as the result of gravity creeping induced by the earthquake.

Key words: fallen stalactite; damaged speleothem; speleoseismology; Wenchuan earthquake

1. Introduction

Speleothems are cave deposits forming from dripping of mineral-rich water. They are quite common in karst landforms and include stalagmites, stalactites and flowstones, etc. Speleothems are usually regarded as good proxies for high-resolution palaeoclimatic reconstructions, in that carbon and oxygen isotopes preserved in speleothems document climatic oscillations throughout the Quaternary (Wang, 2001; Tan et al., 2006; Fairchild et al., 2006; Calaforra et al., 2008; Sorin et al., 2010). In tectonically active regions, deposition of speleothems is sometimes interrupted by earthquakes, forming damaged speleothems that are usually called as speleoseismites. Therefore, speleothems have also been used for palaeoseismic research (Forti, 2001; Lacave et al., 2004; Kagan et al., 2005) and a concise overview of this topic has been given by Forti and Postpichl (1984) and Becker et al., (2006). Earthquake-related speleoseismites include deformed (broken or offset) (stalactites and stalagmites) (Lemeille et al., 1999; Delaby, 2001; Šebela, 2008), irregular stalagmite growth (Postpischl et al., 1991; Forti, 2001; Shao et al., 2014; Rajendran et al., 2016), cave sediment deformation, rock falls in caves, fault displacement in cave walls and ceilings (Becker et al., 2006; Forti, 2007; Camelbeeck et al., 2012; Camelbeeck et al., 2018), and the termination and re-initiation of stalagmite growth (Panno et al., 2009; Shao et al., 2014; Panno et al., 2016).

Whilst deformed speleothems in cave environments are ideal proxies for palaeoseismological study since earthquake-related damages are usually fossilised by calcification with minimal erosion (Forti and Postpischl, 1984; Gilli, 1999; Méjean et al., 2015), few relevant studies have been reported (Cadorin et al., 2001; Gilli, 2004) and how to extract information of paleoseismicities from deformed speleothems remains disputed. For instance, some researchers (Cadorin et al., 2001; Lacave et al., 2004; Szeidovitz et al., 2008; Gribovszki et al., 2017) regarded that broken speleothems could be used to measure fault offsets during earthquakes; whereas others suggested that, except small soda straws, speleothems usually require high acceleration of ground velocity to break, which may bring uncertainties to the offset measurements (Kagan et al., 2005; Panno et al., 2009). Besides the earthquakes, there are some other factors that could cause speleothems to deform, such as human and animal activities, sediments and/or ice creeping, their own gravity and destructive floods, etc. (Gilli, 2004; Becker et al., 2005). Therefore, detailed observations of recent seismic activity are required to determine whether or not broken or deformed speleothems can be used as effective proxies for palaeoseismic investigations. The 2008 Mw 7.9 Wenchuan earthquake provides an excellent opportunity to investigate the relationship between earthquakes and speleothem damage.

The aim of this study is to use field-based evidence to establish whether speleothems record seismic activity. To this end, surveys have been conducted at over a dozen caves near Beichuan County following the 2008 Mw 7.9 Wenchuan earthquake, as this provides an ideal opportunity to assess the sensitivity of the speleothems within the affected cave systems to seismic activity. Local witnesses provided vital information confirming which speleothems sustained earthquake damage. In this paper, five caves were selected to represent the results of the field

investigations. The objectives of this study are: (1) to analyze the major characteristics of damaged speleothems from the earthquake and (2) to discuss the relationship between earthquakes and damaged speleothems in general.

2. Geological setting

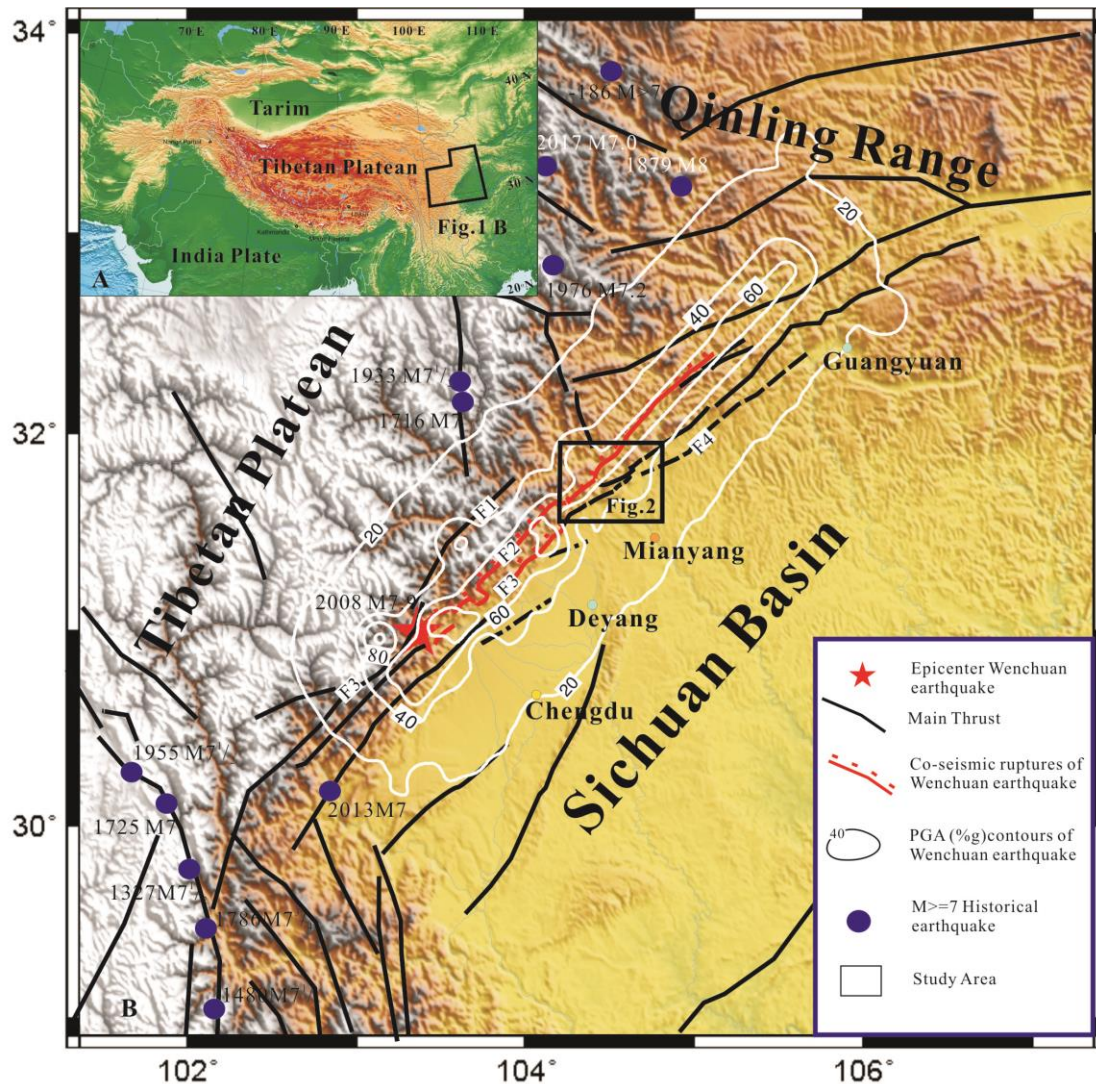


Fig. 1. Co-seismic surface rupture and peak ground acceleration (PGA) contours of the Wenchuan earthquake. The map also shows the structure and history of earthquakes on the Longmen Shan fault zone and its surroundings. The thick red lines mark the co-seismic surface ruptures of the 2008 Wenchuan earthquake (Liu-Zeng et al., 2009; Liu-Zeng et al., 2017). The red star indicates the epicentre of the 2008

Wenchuan earthquake. Other major faults are shown in black. Contours show variations in the horizontal component of PGA (after USGS, 2008). Inset map shows the topography of the Tibetan Plateau and surrounding area. F1=Wenchuan-Maowen fault; F2=Yingxiu-Beichuan fault; F3=Pengguan fault; F4=The Guangyuan-Dayi blind fault

The Longmen Shan is an approximately 500-km-long NE-SW trending mountain range located on the eastern margin of the Qinghai-Tibet Plateau. It marks the steep topographic transition from the high eastern edge of the Tibetan Plateau (~4000–5000 masl) to the significantly lower Sichuan Basin (~500 masl; Fig. 1) (Clark and Royden, 2000; Godard et al., 2009; Liu-Zeng et al., 2011). Within the Longmen Shan are three major NE-SW trending fault zones, and from northwest to southeast they are the Wenchuan-Maowen fault (F1), the centrally positioned Yingxiu-Beichuan fault (F2), and the Pengguan fault (F3) along the southeastern boundary (Burchfiel et al., 1995; Chen and Wilson, 1996; Fu et al., 2011).

At 14:28, May 12, 2008, the Wenchuan earthquake of magnitude Mw 7.9 struck the Sichuan Province, with the epicentre located to the south of Yingxiu town, near Sanjiang Kou (31.0°N, 103.4°E). It caused severe losses both to human lives and the economy, and was one of the most catastrophic earthquakes in China over the past century (Chen et al., 2009). This earthquake was directly attributed to tectonic activity of the Longmen Shan fault zone. Extensive damages occurred over a region that was almost 300 km long and 50 km wide. Significant ground shaking caused by the earthquake was felt up to 1500 km away. Field investigations and remote sensing mapping from satellite images revealed two major surface rupture zones caused by the Yingxiu-Beichuan (F2) and Pengguan (F3) during earthquake (Li et al., 2008; Lin et al., 2009; Xu et al., 2009; Liu-Zeng et al., 2009; Liu-Zeng et al., 2012) (Fig. 1). As

shown in Figs. 1 and 2, peak ground acceleration (PGA) contour lines are elongate ellipses centred on the coseismic surface rupture zone, showing that strong ground motion attenuated with increasing distance away from the ruptured faults (Liu-Zeng et al., 2009).

Our study area is located in the northeastern portion of the Wenchuan earthquake rupture zone (Fig. 1), where the PGA was generally in the range of 30–70%g and locally as high as 80%g. The region between the Yingxiu-Beichuan (F2) and the Pengguan (F3) faults is mainly composed of Devonian to Triassic schist, configured into the box-shaped, NE-trending Tangwangzhai syncline cored by the Carboniferous (Fig. 2). This syncline is about 60 km long, 5~13 km wide, and is geometrically asymmetric. The northwestern limb is well preserved and gently dips to the southeast with an angle $<30^\circ$; whereas the southeastern limb is steeper and clearly cut by several secondary faults. The region to the southeast of the Pengguan Fault (F3) consists of Jurassic, Cretaceous and Cenozoic rocks with locally exposed Triassic (Fig. 2b). The Guangyuan-Dayi blind fault (F4) exists to the east of the Pengguan fault (F3), and is tectonically active according to its geomorphological expressions (Lu et al., 2014) (Fig. 2). Co-seismic ruptures caused by the Beichuan-Yingxiu fault (F2) are clear in the study area; however, those by the Pengguan fault (F3) and the Guangyuan-Dayi blind fault (F4) did not develop. The geomorphology along the margins of the fault differ greatly, with mountains in the northwest and plains and hills in the east.

According to the topography and the distribution of the Devonian-Triassic carbonate rocks (limestone and dolomite) in the study area (Fig. 2c), karstic landforms usually developed in three zones with various topographic and geological features. The western high-mountainous zone (Zone I in Fig. 2a) occurs between 1600

~ 2000 m and is located in the core of the Tangwangzhai syncline. The Devonian and Carboniferous limestone is the major host rock for the karstic landforms in this zone. The central transition zone occurs between 800 ~ 1400 m and comprises the southeastern limb of the Tangwangzhai syncline where numerous faults have developed. The karstic landforms in this zone are usually seen in the Devonian, Permian and Triassic limestone. The eastern basin zone is positioned between 600 ~ 800 m and includes the area on both sides of the Pengguan Fault (F3). The host rocks for the karstic landforms are primarily Triassic limestone. Due to the intense tectonic deformation, the thick carbonate rocks in the study area are conducive to groundwater enrichment, runoff and dissolution, forming distinctive karst landforms. At least 20 large karstic caves have been discovered in this area (Liu et al., 2013), amongst which are the Buddha, Ape King, Crane, Jinguang, Yinguang, Lingquan caves. These karst caves can be divided into three elevation zones (1800 m, 1400 m, 600 m, Fig. 2c).

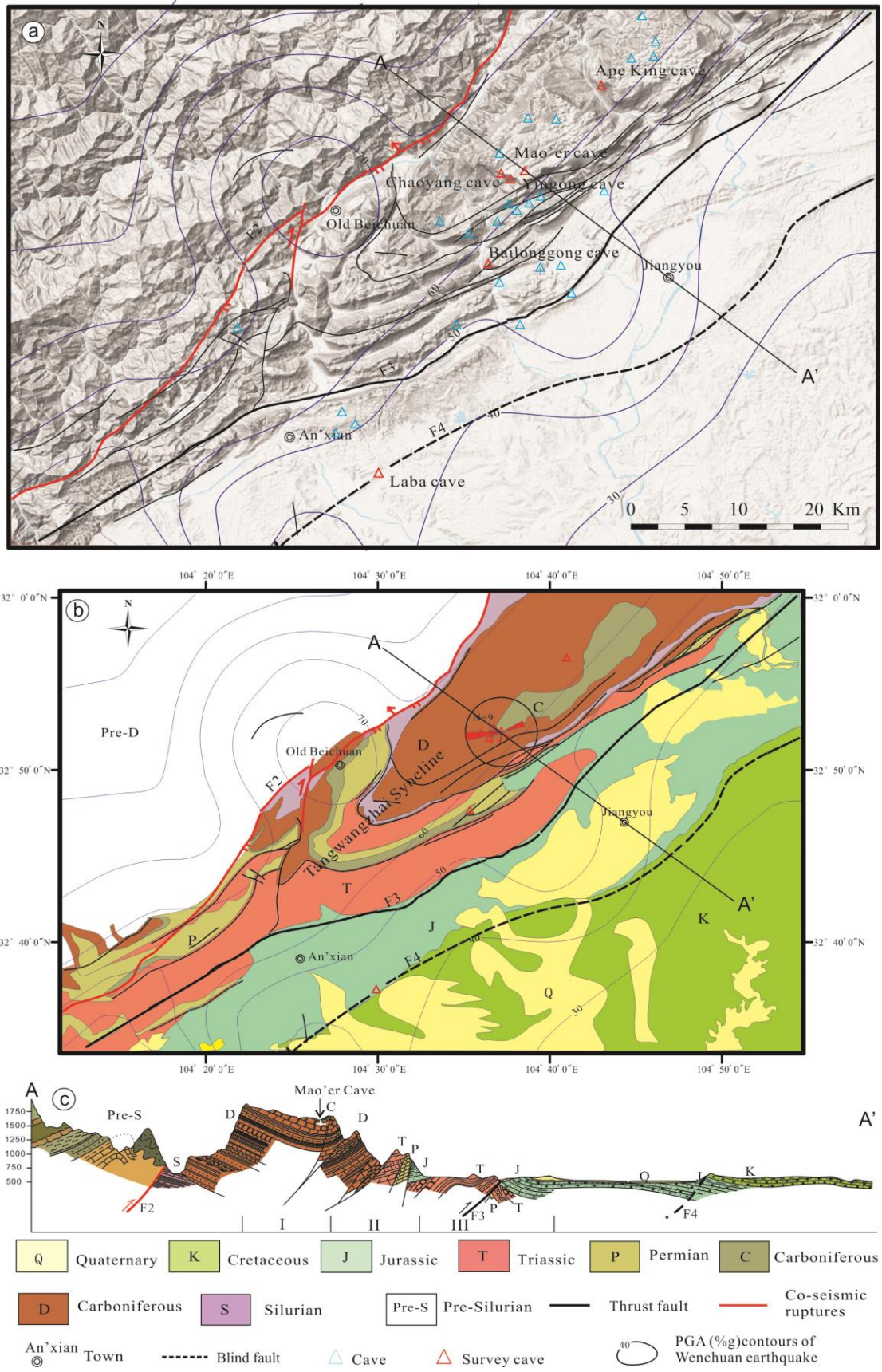


Fig. 2. (a) Shaded relief and simplified tectonic map of the study area. (b) Simplified

geological map of the study area (from the 1:200000 China Regional Geological Survey Report, (Sichuan Bureau of Geology, 1970)). (c) Geological profile across the main structure of the study area. It shows that the geomorphology of karst cave in the study area can be divided into three zones: I = the western high mountain zone; II = the central transition zone and III = the eastern basin zone. The thick red lines mark the co-seismic surface ruptures of the 2008 Wenchuan earthquake. The red triangles indicate the five typical caves described in this study. The contour map shows variations in the horizontal component of PGA (after USGS, 2008). The inset rose diagrams illustrate the preferential SWW-orientation of fallen stalactites. The map location is shown in Fig. 1.

3. Methods and data

We have conducted multiple field surveys of deformed speleothems in karstic caves near Beichuan County from late 2008 through to 2019 (Fig. 2). These caves are all located where peak ground acceleration (PGA) reached 40–70 (%g) during the Wenchuan earthquake and are within 6.5 km away from the seismogenic Yingxiu-Beichuan faults. Since natural or anthropogenic mechanisms are potentially responsible for speleothem collapses or breaks (Gilli, 2004; Becker et al., 2005), caution is required so as not to simply regard all of the damaged speleothems as a direct result of the Wenchuan earthquake, especially when documentation of previous earthquakes is lacking. However, due to the high population density in the study area, there are many local residents who had visited the caves before the earthquake and witnessed the deformation of the speleothems during the earthquake. We thus sorted out the relative timings of speleothem damages related to the Wenchuan earthquake by investigating whether they were newly collapsed or broken in the field with the assistance of these local residents.

Fallen stalactites and stalagmites resulting from earthquakes can normally be linked to seismic parameters. However, there are several variables to consider including ground acceleration, speleothem type controlling sensitivity to seismic shifts, as well as the location within a given cave. During the surveys, in order to investigate the relationship between speleothem damage and earthquake motion, different morphological parameters of the damaged speleothems were measured including the fall direction, height and displacement of broken stalactites (Fig. 3). Among the sixty-one fallen stalactites that were obtained from the Mao'er cave, only nine of them can confidently be confirmed that they were damaged in the 2008 Wenchuan earthquake, according to the nearby villagers. Therefore, these stalactites were collected for further analysis (Tables. 2 and 3).

More than 200 sites in a dozen of the caves have been investigated in the study area. Speleothems were classified into five categories according to their morphological character: (i) spindle shaped; (ii) soda straw; (iii) slender; (iv) weak crystallinity; and (v) stalactite-stalagmite system (Fig. 3d). Here, five example caves located in the city of Mianyang are selected for this study due to their association within areas of different PGA values (Table 1, Fig. 4), e.g. (i) Laba cave 40-50 %g; (ii) Bailonggong cave 50-60 %g; and (iii) Ape King, Mao'er and Yingong caves 50-60 %g.

Table 1 Location of typical caves studied in this paper

Cave	latitude (N)	longitude (E)	altitude (m)	depth* (m)	PGA(%g)
Ape King	31°55'32.68"	104°40'54.96"	1145	200~250	60~70
Mao'er	31°51'24.15"	104°37'07.07"	1607	100~150	60~70

Yingong	31°51'02.67"	104°36'25.49"	1303	350~400	60~70
Bailonggong	31°47'12.40"	104°35'04.41"	588	100~300	50~60
Laba	31°36'46.52"	104°29'59.00"	555	5~30	40~50

*Depth is the thickness of limestone above the cave.

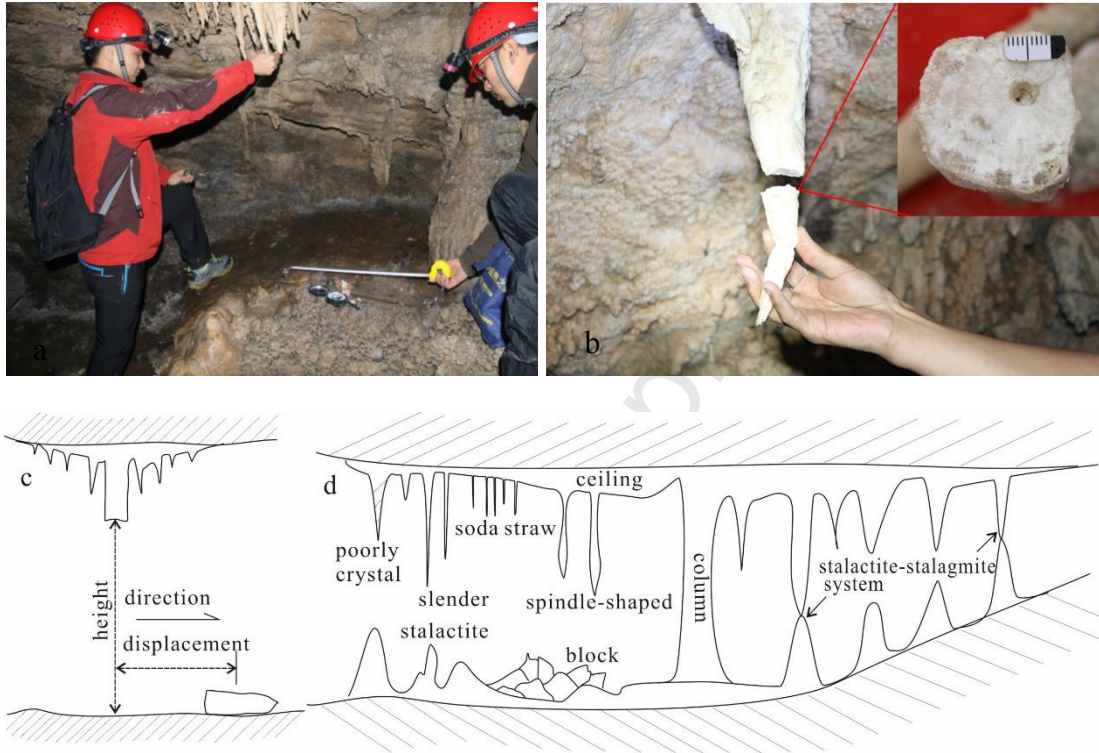


Fig. 3. Photographs detailing the method used to measure the broken stalactites (a) and (b); (c) measurement parameters; (d) sketch of the cave system with the different speleothem features. Illustration: Weak crystallinity is a stalactite in which calcite crystal texture is either sheet, column or needle, and the aggregate is a radial, or one containing impurities, leading to low or weak crystallization. A slender stalactite is a stalactite with a ratio of length to diameter of > 7 . A soda straw is a stalactite which grows downwards from the ceiling, forming a hollow thin calcite tube of uniform width. A spindle-shape is a stalactite with the shape of a spindle, where the upper part is larger than its lower part. If stalagmites and stalactites have been connected, it is called a column. If not, it is called a stalagmite-stalactite system.

Fig. 4. Plan view maps of the five example caves showing the passage morphology of the photo locations.

Table 2a Statistics of the length and diameter of fallen stalactites in the Mao'er cave

No.	Length (cm)	Diameter (cm)				L/D [#]	Note
		Upper (D _{max})	Upper (D _{min})	Below (d _{max})	Below (d _{min})		
1	18.1	3.5	3.5	2.1	2.1	12.9	*
2	18	6	4	2.5	2.4	7.1	*
3	17.4	4.4	3.6			4.4	PC*
4	13	4.5	1.9			4.1	SP*
5	12.9	3.8	2.4			4.2	PC*
6(1)	8.5	3.6	3.5	1.9	1.2	4.3	*
7(2)	5.2	1.9	1.2			3.9	*
8	6.3	1.7	1.5			3.9	SP*
9	10.7	3	2.3			4.0	SP*
10	8.6	1.1	1.1			7.8	*
11	13.15	6	6			2.2	SP
12	4.05	5	5			0.8	
13	4.75	0.55	0.55			8.6	SS
14	7.15	1.25	1.25	1.03		9.7	G-S
15	6.85	1.3	1.3	1		8.6	G
16	12.5	6	6			2.1	SS
17	4.7	0.9	0.9			5.2	SS
18	4.25	0.65	0.65			6.5	SS
19	2.5	0.8	0.8			3.1	S
20	7.55	1.3	1.3			5.8	
21	4.15	0.9	0.9			4.6	SS
22	2.7	0.6	0.6			4.5	SS
23	17.5	3.5	3.5	1.6	1.5	9.0	G
24	10.1	2.9	2.55	1.75	1.75	10.4	
25	6.85	4.15	3.3			1.8	PC
26	8.3	3.25	3.15			2.6	
27	8.6	4.35	3.5			2.2	SP
28	7.6	3.15	2.85			2.5	
29	8.55	3.25	2.15			3.2	PC
30	5.85	3	2.35			2.2	
31	5.55	2.3	1.8	1.45	1.25	7.9	
32	6.85	3.25	2.45			2.4	SP
33	6.65	4.55	3.1	2.9	2.15	5.1	
34	4.15	1.55	1.55	1.55	1.55	>20	
35	3.35	3.05	1.7	1.55	1.25	3.4	
36	3.65	1.05	1.05			3.5	SP
37	4.25	2.05	1.9			2.2	
38	10	4.5	2.95	2.7	3	11.4	

39	4.65	3.35	2.25	2.6	1.9	8.5	
40	45.9	1.55	1.53			29.8	G
41	14.05	2.3	1.65	2.1	1.78	>20	
42	14.79	2.21	1.63	2.08	1.73	>20	
43	34.5	7.36	6.53			5.0	
44	11.66	2.86	2.34			4.5	
45	9.51	1.52	1.16			7.1	
46	5.16	2.34	1.69			2.6	
47	7.2	2.34	2.15			3.2	
48	12.74	4.3	3.73	2.35	2.3	7.5	
49	11	3.38	2.62			3.7	
50	6.02	2.32	2.17	2.15	2.07	44.6	
51	8.24	0.83	0.83			9.9	
52	21.2	8.91	4.44	2.49	2.03	4.8	
53	6.94	3.12	2.66			2.4	
54	8.24	3	2.71			2.9	SP
55	7.42	3.38	3.02	1.17	1.17	3.7	
56	33.6	8.38	6.5	7.45	5.38	32.8	
57	33.5	10.94	8.82			3.4	
58	36.4	6.04	5.83			6.1	SP
59	46.3	15.53	9.84	5.2	4.75	6.0	G
60	42.2	13.78	10.1	5.15	4	5.7	G
61	68.4	36.58	37.53			12.9	S*

Table 2b Ratio of length to diameter of fallen stalactites and its distribution interval

Range of L/D	<7	7-20	>20
Count	40	14	6

Note: $D^{\#} = [(D_{max} + D_{min}) - (d_{max} + d_{min})] / 2$. “Upper” is the upper section of broken stalactites; “below” is the lower section of stalactites. Asterisk indicates that the sample is confirmed to be broken from Wenchuan earthquake by locals. ‘G’ indicates that the sample is a damaged stalagmite. SP = spindle-shaped, SS = soda straw, PC = weak crystallinity, and S = stalactite-stalagmite system.

Table. 3 Parameters of broken stalactites in the Mao'er cave

No.	height (cm)	direction(°)	displacement (cm)	weight (g)
1	230	260	145	235.6
2	161.5	270	11	343.5
3	92	68	24	88.8

4	205	65	20	60.7
5	120	190	44	57
6(1)	236	242	19	71
6(2)		315	31	
7	134	135	31	152.7
8	143	285	20	88.2
9	46	263	32	60.7

4. Field observations

4.1. The Ape King cave

The Ape King cave is located in the Jiuhuang mountain scenic area, and structurally within the core of the Tangwangzhai Syncline between the Yingxiu-Beichuan and Pengguan faults. A typical alpine karst system has been developed within the Devonian limestone. Twenty-three alpine karst caves with different characteristics have been discovered within an area of $< 5 \text{ km}^2$. The altitude of cave entrance is about 1145 masl and the passage is 5.8 km (Fig. 4 a). The cave is comprised two levels separated by a drop of 3-6 m (Fig. 4a), including a hall with an area of more than 2500 m^2 and several branches. The length of the longest passage is over 2.5 km. The cave contains abundant speleothems, including stalactites, stalagmites, pillars, curtains, flowstone and travertine terraces.

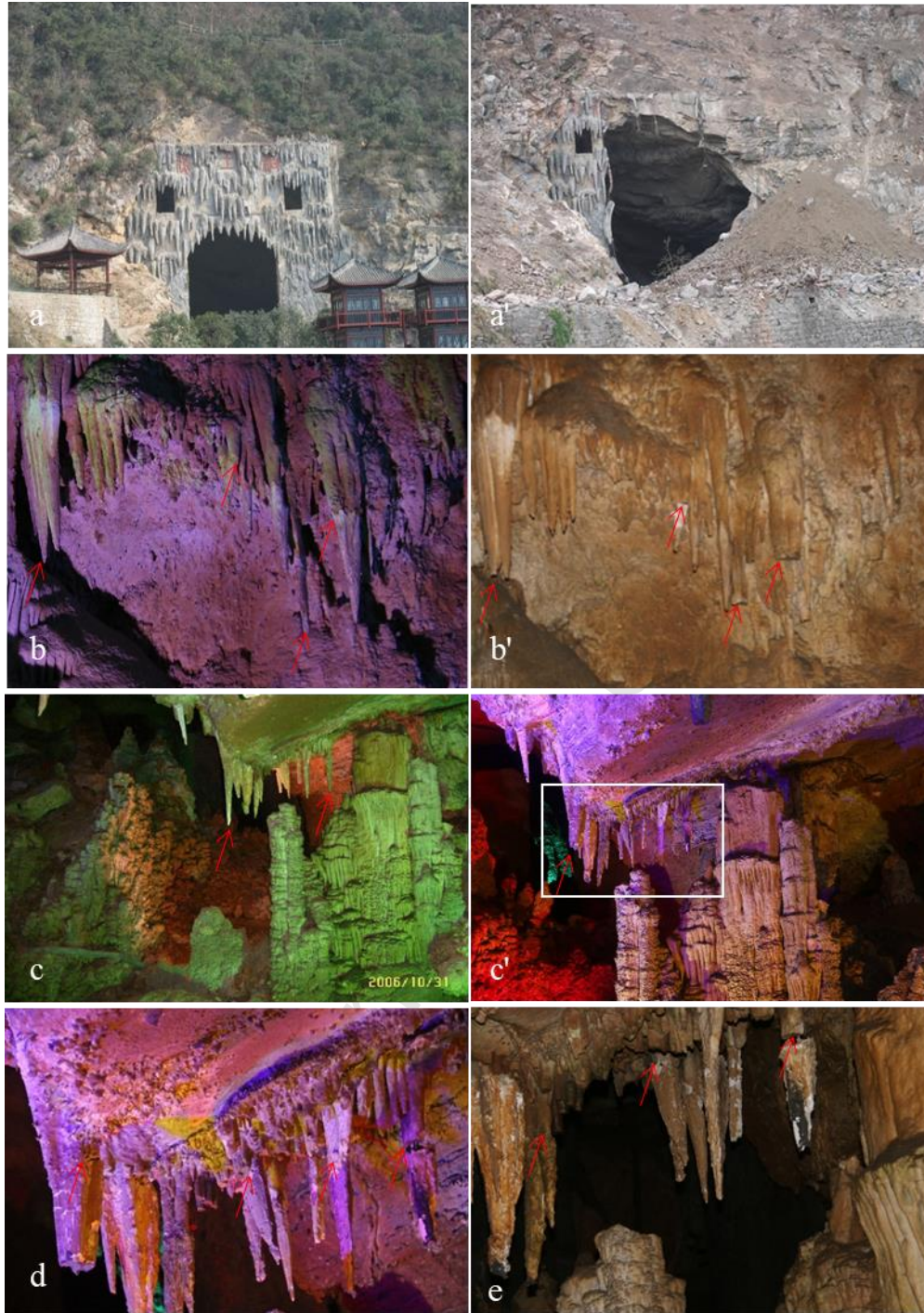


Fig. 5. Ape King cave stalactite photos of before (a-c) and after (a'-c') the Wenchuan earthquake; d and e show broken stalactites during the earthquake that have been re-fixed by the cave staff. The red arrows show damage positions. (a) to (c) are provided courtesy of the local cave staff.

According to officials at the scenic spot, the whole landscape area outside the

Ape King cave was completely destroyed by landslides containing tens of thousands of tons of rock mass (Fig. 5a and a') and about 20% of the stalagmites and stalactites were damaged to varying degrees during the Wenchuan earthquake. The remains of fallen stalagmites and stalactites had been cleaned before our on-site investigation five years later, and some of them have been re-fixed by the staff (Fig. 5d and e). Nevertheless, photos taken before the earthquake (used with permission of the staff: Fig. 5a, b and c) enabled identification of damage related to the earthquake. As shown in Fig. 5, the broken stalactites are characterised by the 'slender' morphological type.

4.2. The Mao'er cave

The Mao'er cave entrance is located on the edge of a cliff on the Wujiahou Mountain with the cave system occurring within the core of the Tangwangzhai Syncline (Fig. 2). The cave is formed within Carboniferous and Devonian limestone and its entrance lies adjacent to a karst sinkhole. The vertical drop from the cave's entrance to the nearest river (Qianjiang River) is >1000 m. The cave has at least four levels that drop consecutively at 3-6 m intervals (Fig. 4b). All levels contain small perennial streams. The length of the longest passage is over 2 km.

The Mao'er cave shows continuous growth of speleothems and many of them were damaged by the Wenchuan earthquake. Two large stalactites fell from the ceiling during the earthquake. The largest one is comprised of five large blocks and debris which covers a total area of at least 2.11 m² (Figs. 6 a-c). The original locations of three of the fallen blocks can be observed on the cave ceiling (Fig. 6d). The relatively smaller block has an area of 0.6 m² (Fig. 6e and f). Many broken stalactites (including soda straws) are well preserved in the Mao'er cave due to the lack of tourists compared to several other sites (Fig. 7). Spindle-shaped stalactites as well as slender soda straws are the most common types of broken stalactite in this cave. Whilst more

than sixty fallen stalactites have been identified, local residents only confirmed that nine of them were definitely broken during the Wenchuan earthquake (Tables 2a and 3).



Fig. 6. Pictures of damaged ceiling stalactite blocks in the Mao'er cave. (a-c) Parts of a ceiling stalactite block with a total area of at least 2.11 m²; (d) three in situ damaged blocks on the ceiling; (e and f) new broken stalactites mixed with old broken stalactites and ceiling rocks.

Fault systems control the passage morphology and overall configuration of the Mao'er cave (Fig.2). Some damaged speleothems are distributed in a faulted area (e.g. Fig. 8), which shows that the stalactites have been broken due to fault activity. For

example, two stalactites have been broken on the side of the fault (Fig. 8a, b) with horizontal movement of approximately 10 cm to the SSE, whilst one of them was broken on the floor (Fig. 8c). Figures 8e and f show two large stalagmites that were broken after being crushed by a stalactite or rock from the ceiling. The orientation of the slope is 335° . Many standing speleothem pillars were observed, with some broken during the earthquake (Fig. 8d). There are also many old ceiling collapses that are mostly covered with stalagmite-stalactite growth (Fig. 8g, h).

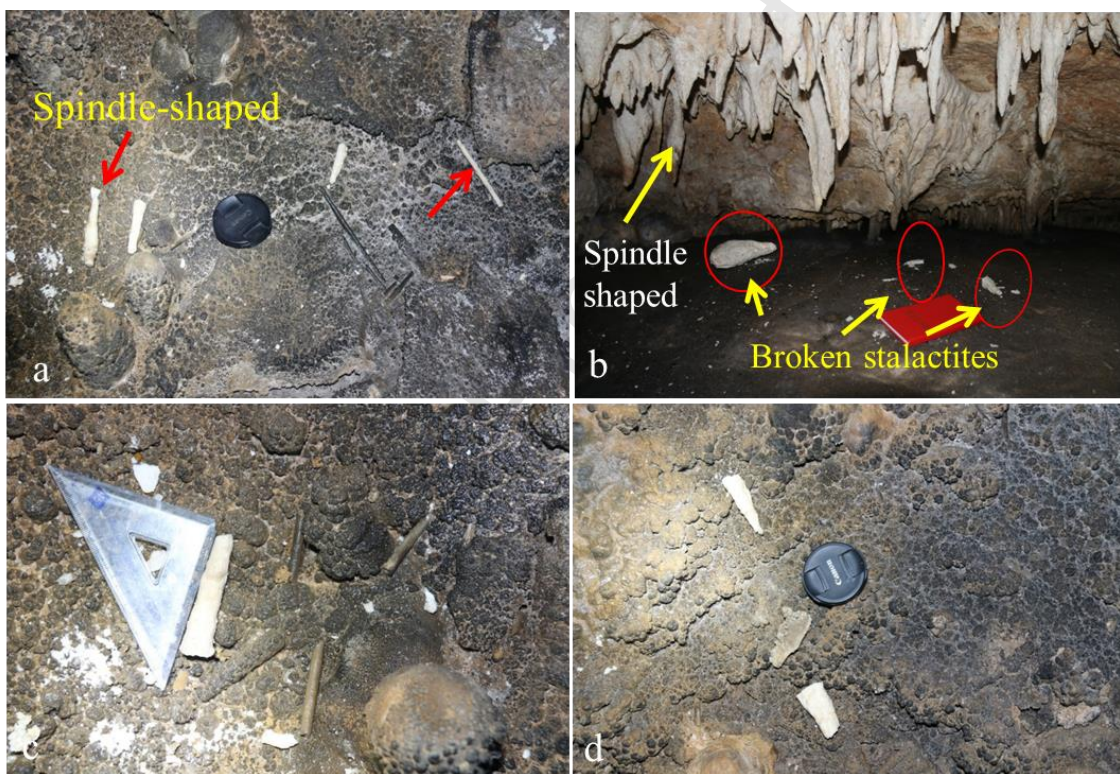


Fig. 7. Pictures of broken stalactites in the Mao'er cave. (a and b) Broken stalactites caused by the 2008 Wenchuan earthquake; (c and d) broken stalactites with uncertain causes. Many old broken stalactites (including soda straws) were also observed (a and c). Cave location is indicated in Fig. 2.



Fig. 8. Pictures of damaged speleothems in the Mao'er cave. (a-c and e-f) Damaged speleothems (stalactites and stalagmites) due to shaking during the Wenchuan earthquake; (d) damaged speleothem pillars; (g-h) old damaged speleothems now covered with stalagmites or stalactites.

4.3. The Yinguang cave

The Yinguang cave is very close to the Mao'er cave, and has developed within Devonian limestone. Its entrance is located on a cliff along the flank of the Wujiahou Mountain (Fig. 2), approximately 1 km away from the Mao'er cave. There are also two other caves in this area. The Jinguang cave is approximately 300 m above the Yinguang cave whilst the Chaoyang cave is approximately 880 m west of the Yinguang cave. The entrance to Chaoyang cave experienced extensive damage during the Wenchuan earthquake. These three caves, including the Mao'er cave, may have developed along the same fault system. Yinguang cave has two natural entrances: (i) a spacious entrance behind an old Taoist building; and (ii) a narrow entrance under the Taoist building with a perennial stream. There is also a waterfall approximately 400 m from the large entrance. The cave has three levels: two dry upper passages and a lower passage containing a perennial stream. The passageway between the two dry passages contains a large pile of fallen rocks (Fig. 4c).

The floor of one of the dry passages consists of flowstone, speleothems, fallen rocks, and one area of soft sediment. The other consists of flowstone, speleothems, fallen rocks, soft sediment, and widespread relics made by nitrates. A large number of damaged speleothems are observed at the end of one dry passage. The Taoist Wang, who is living in the old Taoist building verified which of the speleothems were damaged by the Wenchuan earthquake. There is a stalactite over 40 cm in diameter and a mass of flowstone that formed by ground shaking during the earthquake (Fig.9). Vertical fractures were observed on this broken flowstone. Some new broken stalagmites and stalactites were observed, but whether they were broken by the Wenchuan earthquake remains unknown.

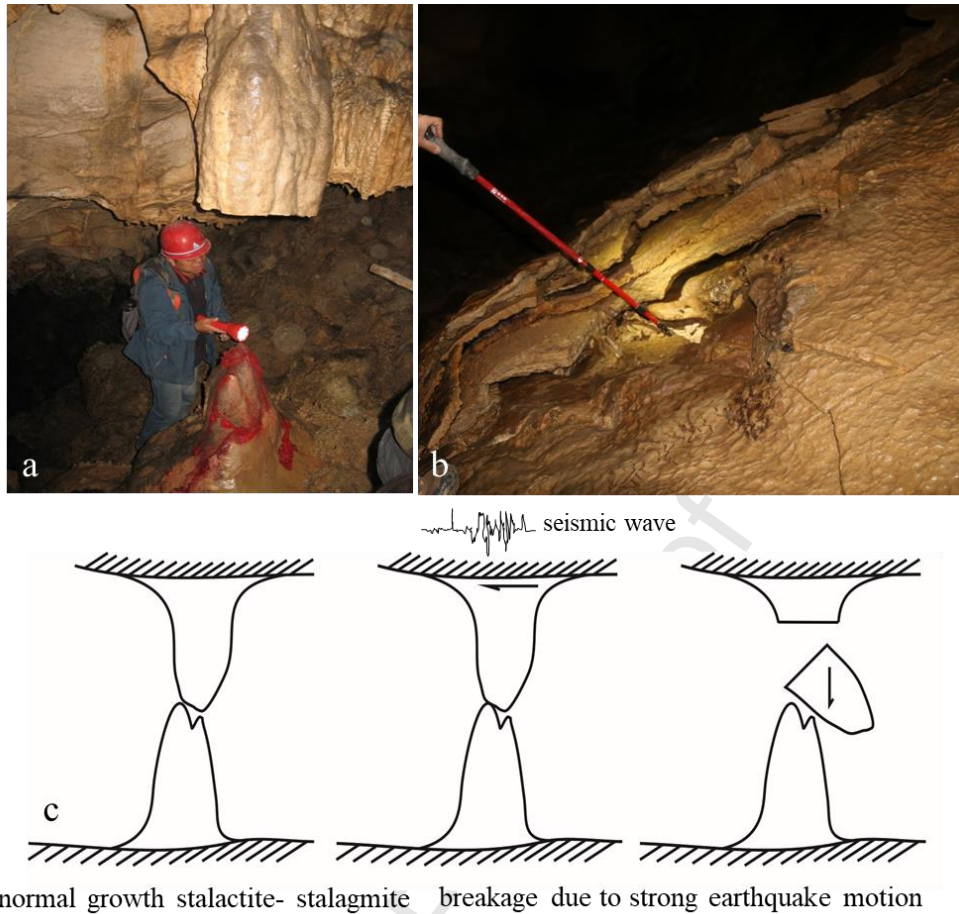


Fig. 9. (a and b) Pictures of damaged speleothems in Yinguang cave; (c) schematic of the main breakage mechanism in the stalagmite-stalactite system.

4.4. The Bailonggong cave

The Bailonggong cave, located to the northwest of Hanzeng town along the east of the Qianjiang River (Fig. 2), is formed within Permian limestone. The cave consists of a main gallery and two secondary branches and is approximately 1.2 km long with a 400-m-long underground river. There are abundant speleothems, including stalactites, stalagmites, pillars, curtains, and travertine terraces (Fig. 4d). As it is a tourist site, there were eye-witness accounts of the damage to the speleothems caused by the earthquake.

Fig. 10 shows three typical cases of damaged speleothems in the Bailonggong Cave, including a bulky stalactite that remains connected to the ceiling at its top but is

faulted towards its base (Fig. 10a). The orientation of the fault surface is 330° . This damage was most likely caused by movement between the roof and the floor, which is consistent with the development of fractures observed in a nearby pillar (Fig. 10b). Multiple broken slender stalactites were observed (Fig. 10c). There are also a dozen traces of broken stalagmites on the approximately 5-m-high ceiling. Although fragments were cleared by workers, old broken stalactites (damaged before the Wenchuan earthquake) are still observed (Fig.10d). The workers confirmed that the broken stalagmites were of the “slender” morphological type.



Fig. 10. Pictures of damaged speleothems in the Bailonggong cave. (a) Broken stalactite caused by movement between the roof and floor; (b) fractures in a pillar; (c)

traces of broken stalagmites; (d) old broken stalagmites.

4.5. The Laba cave

The Laba Cave is located on the southeastern side of Anxian County, in the frontal zone of the Longmen Shan fault zone. The Guangyuan-Dayi blind fault (F4) traverses the cave (Fig. 2). It is a peculiar karst landform formed developed within Late Jurassic calcareous conglomerate (Fig. 2b). The cave consists of a main gallery and a dozen of secondary branches. The main gallery contains a perennial stream, which is linked to a sinkhole 1.3 km from the entrance (Fig. 4e). The floor consists of flowstone, pebbles, speleothems, and soft sediment (Figs. 11a and b). During the earthquake, a collapse occurred in the main passage, approximately 1.1 km from the entrance (Fig. 4e).

There are abundant fractures on the ceiling of the cave, and some are filled with grey black sediments. Some fractures have cut through the cave roof up to the ground surface. A mass of curtain-type stalactites grows underneath the ceiling fractures, which have been damaged by human activities. However, local villagers noted that abundant fractures had appeared in the Laba cave since the earthquake (Fig.11). Based on detailed surveys and according to the appearance and position of the fractures, we classified the fractures into three main types. The first is related to old fractures on wall rock (Fig. 11c). Many stalactites usually grew along the old fractures that had been reactivated during the earthquake. Consequently, the stalactites were damaged and many new fractures developed. The second type appears on the pillars (Fig. 11d) and the last type occurs in the flowstone that are usually vertical or oblique (Fig. 11e).



Fig. 11. Pictures of damaged speleothems in the Laba cave. Floor (a and b), Fractures on (c) the ceiling, (d) the top of a pillar, and (e) the flowstone.

5. Discussion

Speleothem damage due to the Wenchuan earthquake was observed in the northern section of the Longmen Shan fault zone. The study area is approximately 6.5 km away from the co-seismically ruptured faults of the Wenchuan earthquake, which makes it possible to evaluate the extent to which the damaged, fallen, and deformed speleothems resulted from the earthquake. Here, we summarise the patterns of damage or failure of various types of speleothem and analyse the possible reasons for

the damage during the earthquake.

5.1. Major characteristics of damaged speleothems

Collapsed stalactites that had fallen from the ceiling during the earthquake were observed. Typically, seismic waves merely cause additional damage to ceiling stalactite blocks, since the weight and unstable condition of ceiling stalactite blocks plays a decisive role. Fallen stalactites can be classified into five categories according to their shapes (Fig. 3d), amongst which soda straws are the most common type. However, among the 61 broken stalactites in the Mao'er cave (Table 2), forty-one of them have the ratios of length to diameter less than 7, and 8 ones are spindle shaped. Amongst the 9 samples that were confirmed to be broken in the Wenchuan earthquake, three of them are spindle shaped. These observations indicate that spindle-shaped stalactites were more likely to break during an earthquake. There were 20 samples with ratios of length to diameter larger than 7, amongst which 6 were stalagmites. Three samples that were definitely related to the Wenchuan earthquake are the slender-shaped types (with ratios of length to diameter ≥ 7). This indicates that slender-shaped stalactites were easy to break during the earthquake. Moreover, our observations suggested that damage to the stalagmite-stalactite systems likely resulted from a difference of vibration frequency between the roof and floor of the cave during the earthquake (Fig. 9c).

Fractures were also commonly observed in speleothems damaged by the Wenchuan earthquake. They typically exist on the cave ceilings, on the tops of pillars, and within flowstone. There are more fractures in the Laba cave (Fig. 11), which is situated in a PGA range of 40–50 (%g), than in the other caves where higher PGA values of 50–70 were reached (%g). There are three reasons to account for this. First, the Laba cave is closest to the surface, so the speleothems and wall rock are more

heavily weathered than the other caves. Second, the depth of the Laba Cave is only 5~30 m (Table 1), whilst the depths of the other caves are over 100 m. The depth difference is significant since most of a seismic wave's PGA should be attenuated by a factor of about 2.5–3 compared to that at the surface (Gribovszki et al., 2017). Third, the cave is located on the piedmont blind fault (Fig. 2), whose activity may directly promote the development of cave fractures during the earthquake.

5.2. Possible relationship between speleothem damage and earthquake motion

Morphological parameters of damaged speleothems were measured during the field work. Nine typical fallen stalactites, which were confirmed by local residents to have been broken during the Wenchuan earthquake, were measured in situ (Fig. 3). The measured parameters included fallen orientation, height, displacement, and weight (Table 3). Rose diagrams of the fallen stalactite directions showed a preferred SWW-orientation towards Beichuan County where the nearest peak of coseismic surface offsets with respect to the caves occurred (Shen et al., 2009). Due to the motion of the stalactites swing being aligned to the direction of seismic wave propagation, the stalactites could be broken either towards or outwards from the earthquake epicenter. Therefore, we inferred that the direction of fallen stalactites was parallel to the seismic wave propagation. Whilst the morphological parameters of the damaged speleothems indicate multiple earthquake motions, including horizontal ground motion (Cadorin et al., 2001; Szeidovitz et al., 2008; Gribovszki et al., 2017; Rodríguez-Pascua et al., 2017). We propose that the broken stalactites were mainly related to seismic waves due to the findings of this study.

A number of previous studies have shown that damaged speleothems may be indicative of active faults (Gilli, 2005; Becker et al., 2012; Camelbeeck et al., 2012; Briestensky et al., 2014). As shown in Figs. 8b, e, 9a, and 10a, many damaged

speleothems resulted from sudden displacements between the floor and the ceiling during the Wenchuan earthquake. The damage can be illustrated using three examples. Firstly, as shown in Fig. 9 a - c, the stalagmite-stalactite systems were broken due to sudden displacements between the ceiling and floor during the earthquake. The other two cases are stalagmites and stalactites broken by fault movement (Figs. 8b and 10a), with the mechanisms summarised and illustrated in Figs. 12a and b, respectively.

It is notable that all directions of ceiling (hanging wall) movement caused by the Wenchuan earthquake are oriented NW-NNW as this is approximately perpendicular to the strike of co-seismic rupture but opposite to the direction of movement (Liu-Zeng et al., 2009; Wang et al., 2011; Li et al., 2013). An interpretation of this phenomenon is that the faults in the survey caves were not co-seismic structures related to the Wenchuan earthquake. These fault structures were 6.5 km away and accumulated as much as 10–11 m of maximal displacement towards the SE during the earthquake (Ran et al., 2010; Fu et al., 2011). Instead, these faults were likely normal faults as the result of gravity creeping induced by the earthquake (Fig. 12).

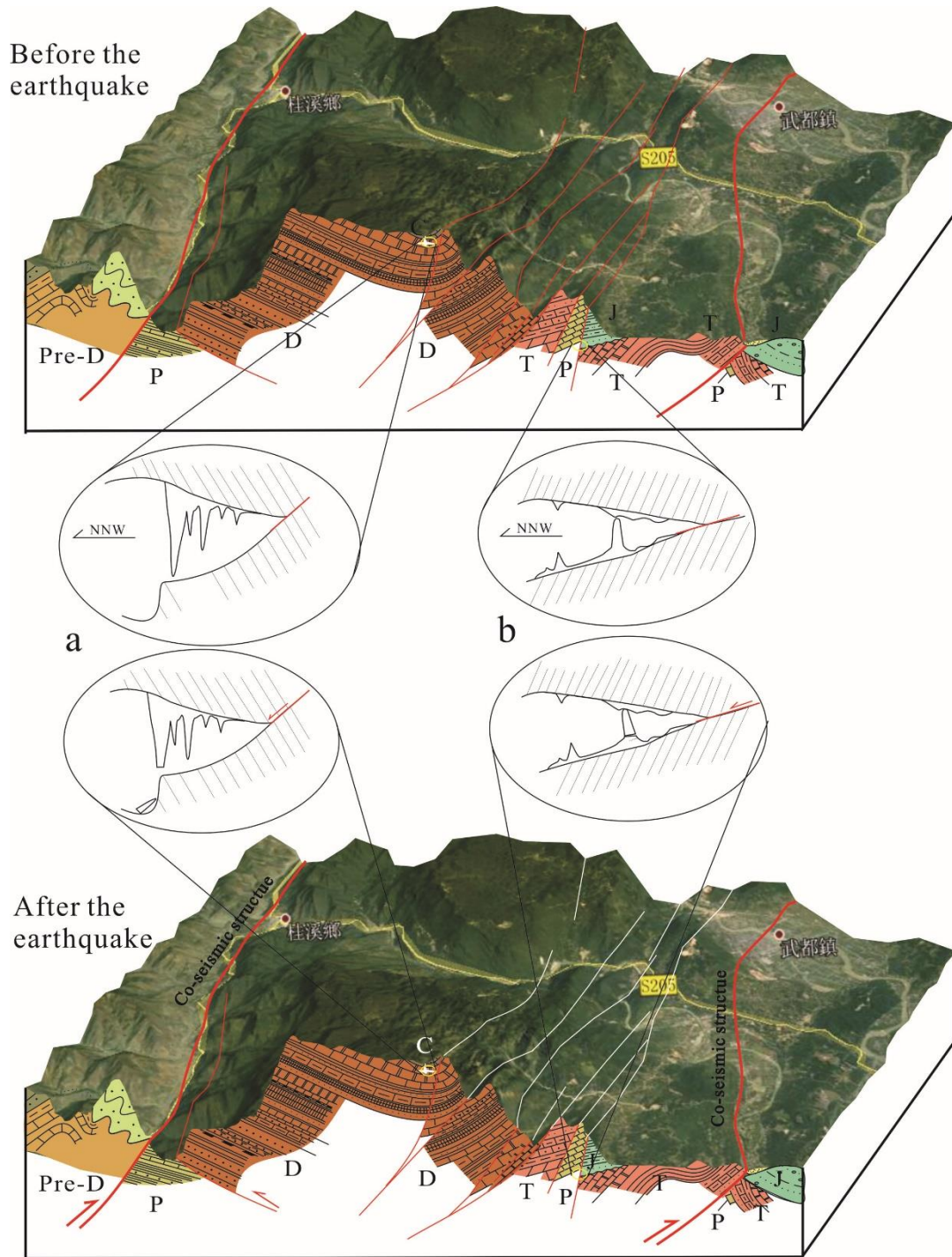


Fig. 12. Models of the damage mechanisms for (a) stalagmites and (b) stalactites during tectonic movement.

6. Conclusions

The use of speleothems as an indicator of palaeoseismic activity has been widely proposed by geologists studying natural caves; however, very few direct observations

have been made to establish the relationship between broken speleothems and strong earthquakes. Herein, we presented a systematic field investigation of damaged speleothems produced by the 2008 Mw 7.9 Wenchuan earthquake in the northern section of Longmen Shan fault zone. Results show that the earthquake caused the caves to collapse either partially or completely. Some collapsed stalactites fell from the ceiling during the earthquake. Soda straws are the most common amongst the fallen stalactites, and our investigation shows that spindle and slender-shaped stalactites are also very likely to break. Fracture formation was a relatively common phenomena during the Wenchuan earthquake and these were typically observed on ceilings, at the top of pillars, and in flowstone. Cave depth may play an important role in fracture development during an earthquake.

Quantification of the orientation of fallen stalactites directions shows that their preferred orientation points towards the nearest centre of surface rupture during the Wenchuan earthquake. We thus suggest that the fallen stalactites were positioned parallel to the propagation direction of the seismic wave. Some of the damaged speleothems resulting from sudden co-seismic movements were observed. The directions of ceiling (hanging wall) movement caused by the Wenchuan earthquake are NW-NNW, which is approximately perpendicular to the strike of co-seismic rupture and consistent with block motion on the footwall of the Yingxiu-Beichuan fault. We consider that faults in these caves are not controlled by co-seismic structures of the Wenchuan earthquake. However, induced by the earthquake, the faults lead to active normal faults or gravity creeping.

Acknowledgements

We thank Wenjie Li, Wen Xu, Dianheng Yang, Jie Wang, Sangui Tang, Taoist Wang and Liulei Bao for their help with the fieldwork. Thanks, are also due to

Tingfang Chen and Bin Liang for helpful discussions and comments on earlier versions of this manuscript. This work was supported by the National Natural Science Foundation of China (grant no. 41672206, 41572035) and the State Key Laboratory of Earthquake Dynamics, Institute of Geology, China Earthquake Administration (grant no. LED2016B07). Financial support for this study was also partially funded by the Project Supported by Scientific Research Fund of Sichuan Provincial Education Department (grant no. 17ZA0394).

References

- Becker, A., Davenport, C. A., Eichenberger, U., Gilli, E., Jeannin, P., Lacave, C., 2006. Speleoseismology: A critical perspective. *Journal of Seismology*, 10 (3), 371-388.
- Becker, A., Ferry, M., Monecke, K., Schnellmann, M., Giardini, D., 2005. Multiarchive paleoseismic record of late Pleistocene and Holocene strong earthquakes in Switzerland. *Tectonophysics*, 400 (1-4), 153-177.
- Becker, A., Haeuselmann, P., Eikenberg, J., Gilli, E., 2012. Active tectonics and earthquake destructions in caves of northern and central Switzerland. *International Journal of Speleology*, 41 (1), 35-49.
- Briestensky, M., Stemberk, J., Rowberry, M. D., 2014. The use of damaged speleothems and in situ fault displacement monitoring to characterise active tectonic structures: an example from Zapadni cave, Czech Republic. *Acta Carsologica*, 43 (1), 129-138.
- Burchfiel, B. C., Zhiliang, C., Yupinc, L., Royden, L. H., 1995. Tectonics of the Longmen Shan and Adjacent Regions, Central China. *International Geology Review*, 37 (8), 661-735.
- Cadorin, J. F., Jongmans, D., Plumier, A., Camelbeeck, T., Quinif, S. D. Y., 2001.

- Modelling of speleothems failure in the Hotton cave (Belgium). Is the failure earthquake induced. *Geologie en Mijnbouw*, 80 (3-4), 315-321.
- Calaforra, J. M., Forti, P., Fernandez-Cortes, A., 2008. Speleothems in gypsum caves and their paleoclimatological significance. *Environmental Geology*, 53 (5), 1099-1105.
- Camelbeeck, T., Quinif, Y., Verheyden, S., Vanneste, K., Knuts, E., 2018. Earthquakes as collapse precursors at the Han-sur-Lesse Cave in the Belgian Ardennes. *Geomorphology*, 308, 13-24.
- Camelbeeck, T., van Ruymbeke, M., Quinif, Y., Vandycke, S., de Kerchove, E., Ping, Z., 2012. Observation and interpretation of fault activity in the Rochefort cave (Belgium). *Tectonophysics*, 581 (SI), 48-61.
- Chen, L., Yuan, X., Cao, Z., Hou, L., Sun, R., Dong, L., Wang, W., Meng, F., Chen, H., 2009. Liquefaction macrophenomena in the great Wenchuan earthquake. *Earthquake Engineering and Engineering Vibration*, 8 (2), 219-229.
- Chen, S. F., Wilson, C. J. L., 1996. Emplacement of the Longmen Shan Thrust-Nappe Belt along the eastern margin of the Tibetan Plateau. *Journal of Structural Geology*, 18 (4), 413-430.
- Clark, M. K., Royden, L. H., 2000. Topographic ooze: building the eastern margin of Tibet by lower crustal flow. *Geology*, 28 (8), 703.
- Delaby, S., 2001. Palaeoseismic investigations in Belgian caves. *Geologie en Mijnbouw*, 80 (3-4), 323-332.
- Fairchild, I. J., Smith, C. L., Baker, A., Fuller, L., Sp Tl, C., Matthey, D., Mcdermott, F., E., I. M. F., 2006. Modification and preservation of environmental signals in speleothems. *Earth-Science Reviews*, 75 (1-4), 105-153.
- Forti, P., 2001. Seismotectonic and paleoseismic studies from speleothems: the state

- of the art. *Geologica Belgica*, 4 (3-4), 175-185.
- Forti, P., 2007. seismotectonic and paleoseismic studies from speleothems. *Geologica Belgica*, 4 (3-4), 175-785.
- Forti, P., Postpischl, D., 1984. Seismotectonic and paleoseismic analyses using karst sediments. *Marine Geology*, 55 (1-2), 145-161.
- Fu, B., Shi, P., Guo, H., Okuyama, S., Ninomiya, Y., Wright, S., 2011. Surface deformation related to the 2008 Wenchuan earthquake, and mountain building of the Longmen Shan, eastern Tibetan Plateau. *Journal of Asian Earth Sciences*, 40 (4), 805-824.
- Fu, G., Shen, X., Fukuda, Y., Gao, S., Yoshii, S., 2011. Co-seismic strain changes of Wenchuan Mw7. 9 earthquake recorded by borehole strainmeters on Tibetan plateau. *Geodesy and Geodynamics*, 2 (3), 42-49.
- Gilli, É., 1999. Evidence of paleoseismicity in a flowstone of the Observatoire cave (Monaco). *Geodinamica Acta*, 12 (s 3-4), 159-169.
- Gilli, É., 2004. Glacial causes of damage and difficulties to use speleothems as palaeoseismic indicators. *Geodinamica Acta*, 3 (17), 229-240.
- Gilli, É., 2005. Review on the use of natural cave speleothems as palaeoseismic or neotectonics indicators. *Comptes Rendus Geoscience*, 337 (13), 1208-1215.
- Godard, V., Cattin, R., Lavé, J., 2009. Erosional control on the dynamics of low-convergence rate continental plateau margins. *Geophysical Journal International*, 179 (2), 763-777.
- Gribovszki, K., Kovács, K., Mónus, P., Bokelmann, G., Konecny, P., Lednická, M., Moseley, G., Spötl, C., Edwards, R. L., Bednárík, M., Brimich, L., Tóth, L., 2017. Estimating the upper limit of prehistoric peak ground acceleration using an in situ, intact and vulnerable stalagmite from Plavecká priepast cave (Detrekői-

- zsomboly), Little Carpathians, Slovakia—first results. *Journal of Seismology*, 21 (5), 1111-1130.
- Hai-Bing, L. I., Zong-Xiu, W., Xiao-Fang, F. U., Li-Wei, H., Jia-Liang, S. I., Zhu-Li, Q., Ning, L. I., Fu-Yao, W. U., 2008. The surface rupture zone distribution of the Wenchuan earthquake (Ms 8.0) happened on May 12th, 2008. *Geology in China*, 35 (5), 803-813.
- Kagan, E. J., Agnon, A., Bar-Matthews, M., Ayalon, A., 2005. Dating large infrequent earthquakes by damaged cave deposits. *Geology*, 33 (4), 261.
- Lacave, C., Koller, M. G., Egozcue, J. J., 2004. What can be concluded about seismic history from broken and unbroken speleothems. *Journal of Earthquake Engineering*, 3 (8), 431-455.
- Lemeille, F., Cushing, M., Carbon, D., Grellet, B., Bitterli, T., Flehoc, C., Innocent, C., 1999. Co-seismic ruptures and deformations recorded by speleothems in the epicentral zone of the Basel earthquake. *Geodinamica Acta*, 12 (3-4), 179-191.
- Li, H., Xu, Z., Wang, H., Si, J., Li, T., Song, S., Pei, J., Guo, L., Sun, Z., 2013. The Principle Slip Zone of the 2008 Wenchuan earthquake: a thrust fault oblique cutting the Yingxiu-Beichuan fault zone. *Geology in China*, 40 (1), 121-139.
- Lin, A., Ren, Z., Jia, D., Wu, X., 2009. Co-seismic thrusting rupture and slip distribution produced by the 2008 Mw 7.9 Wenchuan earthquake, China. *Tectonophysics*, 471 (3-4), 203-215.
- Liu, H., Liu, S., Liu, A., 2013. Characteristics and evaluation of geologic heritage landscape resources in Jiangyou national geopark. *Carsologica Sinica*, 32 (1), 108-116.
- Liu-Zeng, J., Sun, J., Wang, P., Hudnut, K. W., Ji, C., Zhang, Z., Xu, Q., Wen, L., 2012. Surface ruptures on the transverse Xiaoyudong fault: A significant segment

- boundary breached during the 2008 Wenchuan earthquake, China. *Tectonophysics*, 580, 218-241.
- Liu-Zeng, J., Wang, P., Zhang, Z., Li, Z., Cao, Z., Zhang, J., Yuan, X., Wang, W., Xing, X., 2017. Liquefaction in western Sichuan Basin during the 2008 Mw 7.9 Wenchuan earthquake, China. *Tectonophysics*, 694, 214-238.
- Liu-Zeng, J., Wen, L., Oskin, M., Zeng, L., 2011. Focused modern denudation of the Longmen Shan margin, eastern Tibetan Plateau. *Geochemistry, Geophysics, Geosystems*, 12 (11), 1-12.
- Liu-Zeng, J., Zhang, Z., Wen, L., Tapponnier, P., Sun, J., Xing, X., Hu, G., Xu, Q., Zeng, L., Ding, L., Ji, C., Hudnut, K. W., van der Woerd, J., 2009. Co-seismic ruptures of the 12 May 2008, Ms 8.0 Wenchuan earthquake, Sichuan: East–west crustal shortening on oblique, parallel thrusts along the eastern edge of Tibet. *Earth and Planetary Science Letters*, 286 (3-4), 355-370.
- Lu, R., He, D., John, S., Wu, J. E., Liu, B., Chen, Y., 2014. Structural model of the central Longmen Shan thrusts using seismic reflection profiles: Implications for the sediments and deformations since the Mesozoic. *Tectonophysics*, 630, 43-53.
- Méjean, P., Garduño-Monroy, V., Pinti, D. L., Ghaleb, B., Bouvier, L., Gomez-Vasconcelos, M. G., Tremblay, A., 2015. U–Th dating of broken speleothems from Cacahuamilpa cave, Mexico: Are they recording past seismic events? *Journal of South American Earth Sciences*, 57, 23-31.
- Panno, S. V., Chirienco, M. I., Bauer, R. A., Lundstrom, C. C., Zhang, Z., Hackley, K. C., 2016. Possible Earthquakes Recorded in Stalagmites from a Cave in South - Central Indiana. *Bulletin of the Seismological Society of America*, 106 (5), 2364-2375.
- Panno, S. V., Lundstrom, C. C., Hackley, K. C., Curry, B. B., Fouke, B. W., Zhang, Z.,

2009. Major Earthquakes Recorded by Speleothems in Midwestern U.S. Caves. *Bulletin of the Seismological Society of America*, 99 (4), 2147-2154.
- Postpischl, D., Agostini, S., Forti, P., Quinif, Y., 1991. Palaeoseismicity from karst sediments: the "Grotta del Cervo" cave case study (Central Italy). *Tectonophysics*, (193), 33-44.
- Rajendran, C. P., Sanwal, J., Morell, K. D., Sandiford, M., Kotlia, B. S., Hellstrom, J., Rajendran, K., 2016. Stalagmite growth perturbations from the Kumaun Himalaya as potential earthquake recorders. *Journal of Seismology*, 20 (2), 579-594.
- Ran, Y., Shi, X., Wang, H., Chen, L., Chen, J., Liu, R., Gong, H., Gong, H., 2010. The maximum coseismic vertical surface displacement and surface deformation pattern accompanying the Ms 8.0 Wenchuan earthquake. (09), 843-852.
- Rodríguez-Pascua, M. A., Pérez-López, R., Garduño-Monroy, V. H., Perucha, M. A., Israde-Alcántara, I., 2017. Estimation of the epicentral area of the 1912 Acambay earthquake (M 6.9, Mexico) determined from the earthquake archaeological effects (EAE) and the ESI07 macroseismic scale. *Quaternary International*, 451, 74-86.
- Šebela, S., 2008. Broken speleothems as indicators of tectonic movements. *Acta Carsologica*, 37 (1), 51-62.
- Shao, Z., Meng, X., Han, J., Wang, J., Yu, J., He, C., Quan, K., Qi-Guang, C., 2014. Activity of the Longmenshan Tectonic Belt in Sichuan: Evidence from Stalactite Record. *Acta Geoscientia Sinica* (1), 25-30.
- Shen, Z., Sun, J., Zhang, P., Wan, Y., Wang, M., Bürgmann, R., Zeng, Y., Gan, W., Liao, H., Wang, Q., 2009. Slip maxima at fault junctions and rupturing of barriers during the 2008 Wenchuan earthquake. *Nature Geoscience*, 2 (10), 718-

724.

- Sichuan Bureau of Geology. 1970. Regional Geological Survey Report. Mianyang sheet, 1:200000 (in Chinese)[R]. Sichuan Bureau of Geology.
- Sorin, L., Anton, V., Miryam, B., Roi, P., Amos, F., 2010. Late Pleistocene palaeoclimatic and palaeoenvironmental reconstruction of the Dead Sea area (Israel), based on speleothems and cave stromatolites. *Quaternary Science Reviews*, 29 (9–10), 1201-1211.
- Szeidovitz, G., Surányi, G., Gribovszki, K., Bus, Z., Leél-össy, S., Varga, Z., 2008. Estimation of an upper limit on prehistoric peak ground acceleration using the parameters of intact speleothems in Hungarian caves. *Journal of Seismology*, 12 (1), 21-33.
- Tan, M., Baker, A., Genty, D., Smith, C., Esper, J., Cai, B., 2006. Applications of stalagmite laminae to paleoclimate reconstructions: Comparison with dendrochronology/climatology. *Quaternary Science Reviews*, 25 (17-18), 2103-2117.
- USGS, 2008. http://earthquake.usgs.gov/earthquakes/eqinthenews/2008/us2008ryan/finite_fault.ph.
- Wang, Y. J., 2001. A High-Resolution Absolute-Dated Late Pleistocene Monsoon Record from Hulu Cave, China. *Science*, 294 (5550), 2345-2348.
- Wang, Z., Wang, J., Chen, Z., Liu, Y., Huang, R., Pei, S., Zhang, Q., Tang, W., 2011. Seismic imaging, crustal stress and GPS data analyses: Implications for the generation of the 2008 Wenchuan Earthquake (M7.9), China. *Gondwana Research*, 19 (1), 202-212.
- Xu, X., Wen, X., Yu, G., Chen, G., Klinger, Y., Hubbard, J., Shaw, J., 2009. Coseismic reverse- and oblique-slip surface faulting generated by the 2008 Mw 7.9

Wenchuan earthquake, China. *Geology*, 37 (6), 515-518.

Journal Pre-proof

Declaration of competing interests

The authors declare that they have no known competing financial interests or personal relationships that could have appeared to influence the work reported in this paper.

The authors declare the following financial interests/personal relationships which may be considered as potential competing interests:

Highlights

Speleothem damage related to the 2008 Wenchuan (China) earthquake are documented

Damage evidence recorded by field measurement with guidance from local population

Damage includes cave collapse, involving broken stalactites and fracture development

Damage extent and type linked to cave depth and seismic wave propagation

Cave faulting indirectly linked to co-seismic reactivation and gravity collapse

Journal Pre-proof